

New synthetic route to polyphosphine ligands bearing 1,2,4,5-tetrakis(phosphino)benzene framework: structural characterizations of 1,4-(PPh₂)₂-2,5-(PR₂)₂-C₆F₂ (R = Ph, ⁱPr, Et)

Natcharee Kongprakaiwoot, Rudy L. Luck, Eugenijus Urnezisus *

Department of Chemistry, Michigan Technological University, 1400 Townsend Drive, Houghton, MI 49931, USA

Received 31 May 2004; accepted 26 July 2004

Available online 28 August 2004

Abstract

Reactions of 1,4-dibromo-2,5-difluorobenzene with two equivalents of lithium diisopropylamide at low temperature ($T < -90$ °C) followed by a quench with a slight excess of ClPPh₂ afford 1,4-dibromo-2,5-bis(diphenylphosphino)-3,6-difluorobenzene (**1**) in good yields. Reacting **1** with two equivalents of BuLi followed by a quench with a slight excess of ClPR₂ yield novel 1,2,4,5-tetrakis(phosphino)-3,6-difluorobenzenes 1,4-(PPh₂)₂-2,5-(PR₂)₂-C₆F₂ (R = Ph (**2a**); R = ⁱPr (**2b**); R = Et (**2c**)) in moderate yields. Compounds **1** and **2a–c** were characterized by multinuclear NMR spectroscopy and elemental analyses. In addition, molecular structures of **2a–c** have been determined by single crystal X-ray crystallography. Phosphorus atoms of PPh₂/PR₂ substituents in **2a–c** are displaced from the plane of the central phenyl ring due to steric interactions with neighboring groups.

© 2004 Elsevier B.V. All rights reserved.

Keywords: Phosphine ligands; Polyphosphines; Binucleating; Molecular structure

1. Introduction

Tertiary phosphines PR₃ are one of the most widely used ligand classes in transition metal chemistry [1]. Metal complexes with chelating polyphosphine ligands usually have more predictable geometries and better control of the processes at the metal centers [2]. Quite surprisingly relatively few polyphosphine ligands have been used as building blocks for the backbone of coordination polymers [3–6]. Such macromolecules with transition metals in their main chains have attracted considerable attention recently as potentially useful materials with novel physical and chemical properties [7]. Tetrakis(phosphino)benzenes **3a–b** (Fig. 1) have been shown to be effective binucleating ligands in some

transition metal complexes, and as parts of the monomeric units in coordination oligomers and polymers [8–12]. Some of the latter compounds have displayed attractive electrical and optical properties [8,11,13]. However, more detailed spectroscopic and electrochemical measurements have suggested that the metal centers in bimetallic complexes based on **3a–b** lack effective electronic through-ligand coupling due to the absence of a low energy empty ligand-based orbital [14]. In addition, complexes with rigid **3a** usually display rather low solubility [12]. However, fine tuning of the electronic and solubility properties of **3a–b** has not been pursued, as the previously used synthetic methods yielding such ligands did not allow for much variation [8,15].

We have developed a different synthetic route to similar tetrakis(phosphino)benzenes of the general formula 1,4-(PPh₂)₂-2,5-(PR₂)₂-C₆F₂ (Fig. 1, **2a–c**). These compounds resemble **3a–b** in arrangement of phosphino groups, but different properties can be anticipated due

* Corresponding author. Tel.: +1 906 487 2055; fax: +1 906 487 2061.

E-mail address: urnezisus@mtu.edu (E. Urnezisus).

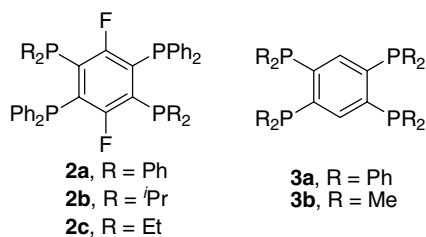


Fig. 1. Polyphosphines with 1,2,4,5-tetrakis(phosphino)benzene framework.

to structural and electronic differences. The presence of the dialkylphosphino functionalities in **2a–c** is expected to render such compounds and their transition metal complexes more soluble in hydrocarbon solvents. The strongly electronegative fluorine substituents on the central phenyl rings in **2a–c** are also expected to directly influence the ligating ability of the P-centers. For example, carbonyl complexes of Cr, Mo and W with structurally related thioethers 1,2,4,5-(SCH₃)₄-C₆F₂ and 1,2,4,5-(SCH₃)₄-C₆H₂ have shown CO stretching frequencies of slightly higher energy for the former, which could be attributed to weaker σ -donor or better π -acceptor properties of the fluorinated ligand [16]. Herein we report the synthetic procedures and structural characterizations of tetrakis(phosphino)benzenes **2a–c**.

2. Results and discussion

When flanked by two halogen atoms, protons in aromatic systems (especially when one of the halogens is fluorine) display “acidity” towards very strong bases [17–20]. Accordingly, the formation of highly reactive (2-bromo-6-fluorophenyl)lithium intermediate upon reaction of lithium diisopropylamide (LDA) with 1-bromo-3-fluorobenzene has been reported [21]. Quite surprisingly, analogous reactivity of difluorodibromobenzenes where each of the remaining two protons is flanked by bromine and fluorine has received rather limited attention and an unsuccessful attempt to deprotonate 1,2-dibromo-4,5-difluorobenzene at -78 °C has been reported [17]. The temperature is a crucial factor in such reactions, and recently we found that double deprotonations of similarly substituted benzenes bearing two “acidic” protons are facile when reactions are conducted at very low temperatures. Thus, 1,4-dibromo-2,5-

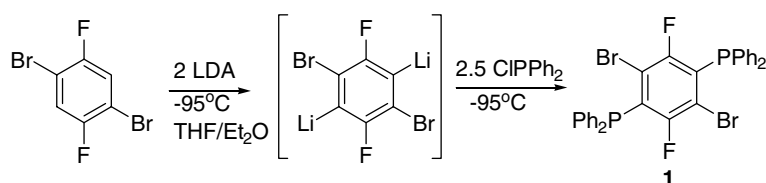
difluorobenzene readily undergoes a double deprotonation with two equivalents of LDA when the reaction media is carefully kept around -100 °C (Scheme 1).

Dilithiotetrahalobenzene thus generated is very unstable thermally and decomposes at temperatures higher than -80 °C. However, if maintained around -95 °C, reactions with electrophiles are possible, and addition of ClPPh₂ (slight excess) produces 1,4-dibromo-3,6-bis(diphenylphosphino)-2,5-difluorobenzene, **1**, in good yields ($\sim 70\%$) (Scheme 1). Analogous reactions of 1,4-dibromo-2,5-difluorobenzene with only one equivalent of LDA followed by ClPPh₂ quench did not result in selective monodeprotonation and exclusive formation of expected (2,5-dibromo-3,6-difluorophenyl)diphenylphosphine, for in addition to this compound, reaction mixtures also contained substantial amounts of **1** and unreacted 1,4-dibromo-2,5-difluorobenzene (ascertained by GC/MS). We have also observed similar reactivities for 1,2-dibromo-4,5-difluorobenzene and 1-bromo-2-chloro-4,5-difluorobenzene [22].

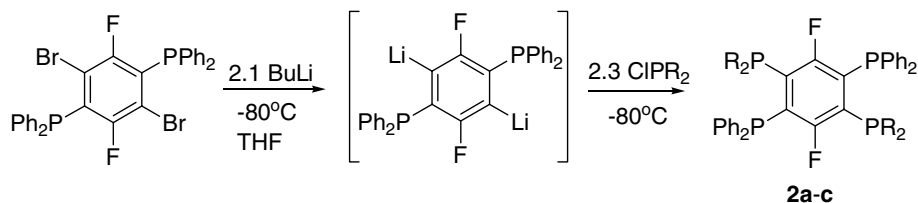
Compound **1** displays NMR (¹H, ³¹P and ¹⁹F) signatures corresponding to the C_{2h} symmetry of the molecule. The magnitude of phosphorus–fluorine coupling (³J_{PF} = 12 Hz, ⁴J_{PF} = 6 Hz) is similar to values observed in structurally related compounds [15]. So far we have not been able to obtain X-ray quality crystals of this material.

The presence of two bromines at ortho positions to the PPh₂ groups makes compound **1** an attractive building block for the syntheses of an entire range of novel binucleating ligands. We found that both bromines are readily displaced utilizing standard alkyllithium/halogen exchange reactions (Scheme 2). Again, the choice of conditions is rather critical, and such reactions are facile only at low temperatures ($T < -80$ °C). The resulting dilithiated intermediate is quite unstable thermally, and extensive decomposition occurs if the temperature is allowed to reach -60 °C and above. However, if the reaction mixtures are quenched with an excess of dialkyl/diarylchlorophosphine before warmup (Scheme 2), pure **2a–c** can be isolated in moderate yields (~ 20 – 40%), although the initial crude yields are higher (~ 50 – 60%).

Tetrakis(phosphino)difluorobenzenes **2a–c** are thermally stable (sharp melting points have been determined), pale yellow (**2a**) to deep yellow (**2b–c**)



Scheme 1.



Scheme 2.

crystalline solids, which are relatively air stable in the solid state, but oxidize in solution if exposed to air. Compound **2a** displays one signal in its ^{31}P NMR spectrum due to the equivalent nature of all four PPh_2 groups in solution. No 3-bond ^{19}F – ^{31}P coupling was observed in both the ^{31}P NMR and the ^{19}F NMR spectra. However, such coupling can be seen in **2b** ($^3J_{\text{PF}} = 13$ Hz), in addition to strong 3-bond P–P coupling ($^3J_{\text{PP}} = 195$ Hz). Such $^3J_{\text{PP}}$ values are typical for mutually ortho P(III) groups, when the lone pairs are directed towards each other [15,23]. A second order ^{31}P NMR spectrum was resolved for **2c**, and a coupling value ($^3J_{\text{PP}} = 198$ Hz) was determined via spectral simulation using *g* NMR software [24].

Single crystals of **2a–c** were obtained during low temperature (-28 °C) crystallizations under N_2 (from toluene (**2a**) and toluene/hexanes (**2b–c**)). X-ray diffraction experiments allowed the determination of their molecular structures. The final figures of merit and selected

bond distances and angles are summarized in Tables 1 and 2 respectively.

According to the CSD [25], the only other structurally characterized 1,2,4,5-tetrakis(phosphino)benzene prior to our work was 1,2,4,5-tetrakis(diphenylphosphino)benzene (**1a**) [12]. Its closest structural analog among our compounds is **2a** (Fig. 2(a)), as the two differ only by the presence of two fluorine atoms instead of H-atoms on the central phenyl ring of the latter.

Both compounds possess planar central phenyl rings (average carbon atom deviation from the weighted least-squares plane through C1–C2–C3–C4–C5–C6 atoms in **2a** is 0.02 Å). However, the internal angles in the central ring are more distorted in **2a** (C1–C6–C5 = 117.0(6)° to C2–C1–C6 = 126.1(6)°, see Table 2) compared to **3a** where the corresponding values are closer to 120° (118.3(2)–122.6(2)°) [12]. All phosphorus atoms in **3a** are reported to be in the plane of the central phenyl ring and such an arrangement is typically found in other

Table 1

Crystal data for 1,4-(PPh_2)₂-2,5-(PR_2)₂- C_6F_2 (R = Ph, ^iPr , Et) (**2a–c**)

Crystal data	2a	2b	2c
Formula	$\text{C}_{54}\text{H}_{40}\text{F}_2\text{P}_4$	$\text{C}_{42}\text{H}_{48}\text{F}_2\text{P}_4$	$\text{C}_{38}\text{H}_{40}\text{F}_2\text{P}_4$
Formula weight	850.74	714.68	658.58
Space group	$P2_1/c$	$P2_1/c$	$P\bar{1}$
<i>a</i> (Å)	10.700(2)	10.576(2)	8.441(2)
<i>b</i> (Å)	18.689(5)	11.927(3)	9.805(3)
<i>c</i> (Å)	22.272(5)	16.405(3)	11.885(3)
α (°)	90	90	74.29(2)
β (°)	97.21(2)	107.18(2)	89.06(2)
γ (°)	90	90	72.69(2)
<i>V</i> (Å ³)	4418.6(18)	1977.0(7)	901.8(4)
<i>Z</i>	4	2	1
ρ_{calc} (g/cm ³)	1.279	1.201	1.213
μ (Mo <i>K</i> α , mm ⁻¹)	0.216	0.228	0.245
<i>T</i> (K)	295(2)	295(2)	295(2)
λ (Å)	0.71073	0.71073	0.71073
θ Range (°)	1.00–22.50	1.00–22.50	1.00–25.00
Final <i>R</i> indices [<i>I</i> > 2 σ (<i>I</i>)] ^a	$R_1 = 0.066$, $wR_2 = 0.103^{\text{b,c}}$	$R_1 = 0.055$, $wR_2 = 0.086^{\text{b,d}}$	$R_1 = 0.036$, $wR_2 = 0.095^{\text{b,e}}$
<i>R</i> indices (all data)	$R_1 = 0.255$, $wR_2 = 0.148$	$R_1 = 0.175$, $wR_2 = 0.115$	$R_1 = 0.050$, $wR_2 = 0.102$
Largest difference peak and hole	0.375, –0.269	0.218, –0.265	0.300, –0.253
Goodness-of-fit on F^2	1.011	1.006	1.051

^a $R_1 = \sum(F_o - F_c) / \sum(F_o)$.^b $wR = [\sum[w(F_o^2 - F_c^2)^2] / \sum[w(F_o^2)^2]]^{1/2}$.^c $w = 1/[\sigma^2(F_o^2) + (0.0378 * P^2 + 1.2185 * P)]$, where $P = (F_o^2 + 2 * F_c^2) / 3$.^d $w = 1/[\sigma^2(F_o^2) + (0.0147 * P^2 + 2.2478 * P)]$, where $P = (F_o^2 + 2 * F_c^2) / 3$.^e $w = 1/[\sigma^2(F_o^2) + (0.0485 * P^2 + 0.2806 * P)]$, where $P = (F_o^2 + 2 * F_c^2) / 3$.

Table 2
Selected bond distances and angles for **2a–c**

	2a	2b	2c
<i>Bond distances (Å)</i>			
C1–C2	1.392(8)	1.394(6)	1.384(2)
C2–C3	1.420(8)	1.404(6)	1.405(2)
C3–C4	1.410(8)	1.383(6) ^a	1.387(2) ^a
C4–C5	1.381(8)		
C5–C6	1.424(8)		
C1–C6	1.365(8)		
F1–C1	1.361(7)	1.359(5)	1.3571(19)
F2–C4	1.353(7)		
P1–C2	1.853(7)	1.848(5)	1.8520(18)
P2–C3	1.846(7)	1.844(5)	1.8557(18)
P3–C5	1.863(7)		
P4–C6	1.855(6)		
<i>Bond angles (°)</i>			
F1–C1–C6	117.5(6)	116.7(5) ^b	116.89(15) ^b
F1–C1–C2	116.4(6)	116.9(4)	117.76(14)
C6–C1–C2	126.1(6)	126.4(4) ^b	125.32(16) ^b
C1–C2–C3	117.5(6)	117.5(4)	117.32(15)
C1–C2–P1	124.9(5)	122.1(4)	124.57(13)
C3–C2–P1	117.5(5)	119.8(4)	117.87(13)
C4–C3–C2	116.1(6)	116.1(4) ^a	117.29(15) ^a
C4–C3–P2	125.8(5)	124.9(4) ^a	124.38(13) ^a
C2–C3–P2	118.0(5)	118.6(4)	118.11(12)
F2–C4–C5	117.9(6)		
F2–C4–C3	116.9(6)		
C5–C4–C3	125.2(6)		
C4–C5–C6	117.7(6)		
C4–C5–P3	123.2(5)		
C6–C5–P3	119.0(5)		
C1–C6–C5	117.0(6)		
C1–C6–P4	126.0(5)		
C5–C6–P4	116.8(5)		

^a C4 represents symmetry generated C1.

^b C6 represents symmetry generated C3.

structurally characterized 1,2-diphosphenobenzenes [23]. The phosphorus atoms in **2a** are shifted from the in-plane positions by 0.199(2)–0.241(2) Å, although the P–C (carbons of the central ring) bond distances remain

within the expected range [26]. The torsion angles P1–C2–C3–P2 (−10.9(8)°) and P3–C5–C6–P4 (−12.2(7)°) are another indicator of this deviation. Such differences between the key structural parameters of **2a** and **3a** can be attributed to steric crowding resulting from the fluorine atoms on the central ring of the former, even though fluorine atoms are not considered bulky substituents. The distortion of the PPh₂ groups (by 0.133 Å) from the plane of the central phenyl ring in 1,4-bis(diphenylphosphino)-2,5-difluorobenzene has been reported [27], as well as similar distortions for the PR₂ groups caused by the steric bulk of adjacent substituents in other related compounds [28,29]. The positioning of the PPh₂ substituents (which are adjacent to a fluorine atom) above and below the plane of the central phenyl ring in **2a** (Fig. 2(b)) renders the Ph groups attached to the same phosphorus atom non-equivalent. Room temperature ¹H NMR spectra of **2a** consist of a complex signal in the aromatic region and further variable temperature studies are necessary to assess the nature of **2a** in solution. Our data on **2b–c** (discussed in later paragraphs) suggests that in solution these molecules closely resemble the structures observed in the solid state.

The presence of the more sterically demanding diisopropylphosphine groups in **2b** (Fig. 3) results in more severe distortions. The values for the internal angles of the planar central phenyl ring remain similar to those observed in **2a** (C3'–C1–C2 = 126.4(4)°, C1–C2–C3 = 117.5(4)°, see Table 2), but the bending of phosphorus atoms away from the plane of the central ring is more severe in **2b** (−0.252(2) Å (P1) and 0.271(2) Å (P2)). Accordingly, the torsion angle P1–C2–C3–P2 at −18.7(6)° is significantly larger than the corresponding angles in **2a**. The non-equivalency of the isopropyl groups resulting from such distortion clearly persists in solution and two ¹H NMR signals for CH₃ groups are observed (δ 1.11 and 0.74), whereas the CH proton produced a complex multiplet (δ 2.34). The combination of

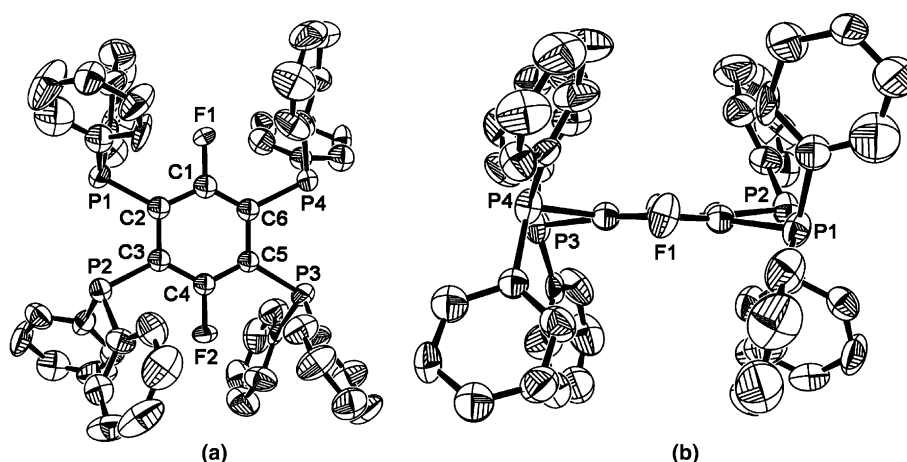


Fig. 2. (a) Molecular structure of **2a** (50% thermal ellipsoids) without H atoms and (b) a view of the molecule along F1–C1–C4–F2 line.

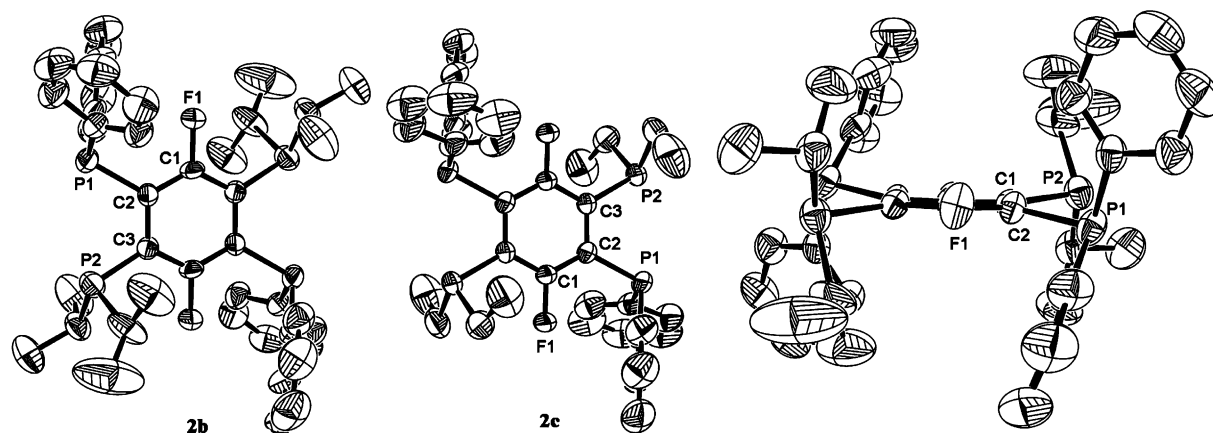


Fig. 3. Molecular structures for **2b** (major orientation only) and **2c** (40% thermal ellipsoids) without H atoms. Illustration on the far right depicts the arrangement of the phosphorus atoms in **2b** relative to the plane of the central phenyl ring. There is a similar arrangement in **2c**.

diphenylphosphino and diethylphosphino groups in **2c** (Fig. 3) produce fewer steric demands, as the distortions from ideal geometry are less pronounced. The central phenyl ring (planar) is still distorted from the ideal geometry ($C2-C1-C3' = 125.32(16)^\circ$, $C1-C2-C3 = 117.32(15)^\circ$), but the displacements of the phosphorus atoms from the plane of the central phenyl ring are smaller than in **2c**: $0.1538(7)$ Å for P1 and $-0.2260(7)$ Å for P2. This accordingly results in a smaller torsion angle ($(P1-C2-C3-P2) = 13.3(2)^\circ$). The non-equivalency of the ethyl groups also persists in solution, but the 1H NMR spectrum of **2c** is not well resolved (at room temperature and 400 MHz) with multiplets for both the CH_3 (δ 0.85) and the CH_2 (δ 1.81) groups; complex multiplets are also produced by phenyl protons in both **2b** and **2c**. Finally, it is noteworthy that the PR_2 groups adjacent to a fluorine atom in **2b** and **2c** distort towards one another, see Fig. 3. This is in contrast to the equivalent groups being on opposite sides of the central phenyl ring in **2a**. This illustrates the flexibility of the phenyl ring as the substituents distort to minimize steric interactions.

3. Experimental

3.1. General procedure

Manipulations requiring inert atmospheres were carried out by using Schlenk techniques or in a dry box under a N_2 atmosphere. Low temperature reactions were performed in Schlenk flasks immersed in hexanes/liquid N_2 slush, contained in a Dewar flask. Solvents were purified before use by distillation from Na-benzophenone ketyl (ether, THF, hexanes) or CaH_2 (toluene, acetonitrile) under N_2 atmosphere. Methanol was deoxygenated by bubbling nitrogen through it for 1 h. Commercially available chlorophosphines $CIPR_2$ were purified prior to use: $CIPPh_2$ was vacuum distilled; $CIPeT_2$ and CIP^iPr_2 were

frozen and degassed while thawing under vacuum (repeated three times). LDA (lithium diisopropylamide) was freshly prepared immediately prior to use according to a published procedure [17]. 1H , ^{31}P , and ^{19}F NMR spectra were recorded on Varian INOVA spectrometer operating at 400, 161, and 376 MHz, respectively. Spectra are referenced to tetramethylsilane (1H), 85% H_3PO_4 (^{31}P) (external reference), and $CFCl_3$ (^{19}F) (internal standard in a sealed capillary tube). Mass spectrometric measurements were performed on a Shimadzu QP5050A instrument. Elemental analyses were performed at Galbraith Laboratories, Inc.

3.2. Syntheses

3.2.1. 1,4-dibromo-3,6-difluoro-2,5-bis(diphenylphosphino)-benzene (**1**)

To a stirred solution of 1,4-dibromo-3,6-difluorobenzene (1.0 g, 3.68 mmol) in THF (120 ml) at $-95^\circ C$ was added (via cannula) freshly prepared LDA (2.0 equivalent) in the same solvent. After stirring for 5 min, a solution of 1.69 ml (2.5 equivalents) of diphenylchlorophosphine in THF (10 ml) was slowly introduced via a cannula. The mixture was stirred at $-95^\circ C$ for 1 h and then allowed to warm up to room temperature overnight. A clear yellowish brown solution was filtered, volatiles removed under vacuo to yield an oily yellow solid. Washings with methanol yielded **1** as a white powder. Yield: 1.65 g (70%). Melting point: $263-264^\circ C$. 1H NMR ($CDCl_3$): δ 7.34 (m). ^{31}P NMR ($CDCl_3$): δ 0.54 (dd, $^3J_{PF} = 12$ Hz, $^4J_{PF} = 6$ Hz); ^{19}F NMR (C_6D_6): δ -88.50 (dd, $^3J_{FP} = 12$ Hz, $^4J_{FP} = 6$ Hz). MS (EI): $m/z = 640$ (M^+). Anal. Calc. for $C_{30}H_{20}Br_2F_2P_2$: C, 56.28; H, 3.15. Found: C, 56.21; H, 3.27%.

3.2.2. 1,2,4,5-Tetrakis(phosphino)-3,6-difluorobenzenes 1,4-(PPh_2) $_2$ -2,5-(PR_2) $_2$ - C_6F_2 (**2a-c**)

Compounds **2a-c** were prepared by the same synthetic protocol. To a stirred solution of 1,4-dibromo-

3,6-difluoro-2,5-bis(diphenylphosphino)benzene (1.00 g, 1.56 mmol) in 120 ml THF at $-80\text{ }^{\circ}\text{C}$ was added *n*-BuLi (2.1 equivalent) as a 1.6 M solution in hexanes. The mixture was stirred for 1 h at $-80\text{ }^{\circ}\text{C}$, and then was treated with a solution of 2.3 equivalents of the corresponding ClPR_2 in 10 ml of THF. After stirring for another hour at $-80\text{ }^{\circ}\text{C}$ the mixture was allowed to warm up to room temperature overnight.

3.2.3. 1,2,4,5-(*PPh*₂)₄-C₆F₂ (**2a**)

The reaction mixture contained pale yellow precipitate, which was filtered off and extracted with toluene (70 ml).

The extract was filtered, the filtrate was placed at $-28\text{ }^{\circ}\text{C}$, yielding pale yellow crystals after one week (isolated by filtration). Yield: 1.07 g (40%). Melting point: 274–276 $^{\circ}\text{C}$. ¹H NMR (CDCl₃): δ 7.19 (m). ³¹P NMR (CDCl₃): δ -11.31 (s); ¹⁹F NMR (C₆D₆): δ -78.53 (s). MS (EI): *m/z* = 850 (M⁺). Anal. Calc. for C₅₄H₄₀F₂P₄: C, 76.23; H, 4.74. Found: C, 74.92; H, 4.72%. (Results consistently low on carbon were obtained on repeated runs on two different batches of the material. Multinuclear NMR and GC/MS spectroscopic characterizations revealed no impurities.)

3.2.4. 1,4-(*PPh*₂)₂-2,5-(*PⁱPr*₂)₂-C₆F₂ (**2b**)

The reaction mixture was filtered, volatiles removed under vacuo to yield an oily yellow solid, which was extracted with a 1:1 mixture of hexanes and toluene (100 ml). Yellow crystals of **2b** precipitated on standing at $-28\text{ }^{\circ}\text{C}$ for one day, and were isolated by filtration. Yield: 0.23 g (20%). Melting point 238–239 $^{\circ}\text{C}$. ¹H NMR (CDCl₃): δ 7.33 (m, 20H), 2.34 (m, 4H), 1.11 (m, 12H), 0.74 (m, 12H). ³¹P NMR (CDCl₃): δ 12.64 (dd, ³*J*_{PP} = 195 Hz, ³*J*_{PF} = 13 Hz), -12.91 (dd, ³*J*_{PP} = 195 Hz, ³*J*_{PF} = 13 Hz). ¹⁹F NMR (C₆D₆): δ -84.32 (s). MS (EI): *m/z* = 714 (M⁺). Anal. Calc. for C₄₂H₄₈F₂P₄: C, 70.58; H, 6.77. Found: C, 70.05; H, 6.92%.

3.2.5. 1,4-(*PPh*₂)₂-2,5-(*PEt*₂)₂-C₆F₂ (**2c**)

This was isolated analogously to **2b**. Yield: 0.21 g (21%). Melting point 198–200 $^{\circ}\text{C}$. ¹H NMR (CDCl₃): δ 7.33 (m, 20H), 1.81 (m, 8H), 0.85 (m, 12H). ³¹P NMR (CDCl₃): δ -11.48 (dm, ³*J*_{PP} = 198 Hz), -12.41 (dm, ³*J*_{PP} = 198 Hz). ¹⁹F NMR (C₆D₆): δ -88.44 (s). MS (EI): *m/z* = 658 (M⁺). Anal. Calc. for C₃₈H₄₀F₂P₄: C, 69.30; H, 6.12. Found: C, 69.22; H, 6.47%.

3.3. X-ray crystallography

In all cases, crystals were removed from the mother liquor, coated with epoxy resin and placed on the head of a thin glass fiber, which was anchored in a goniometer mounting pin. The pin-mounted crystal was then inserted into the goniometer head of the X-ray

diffractometer (Enraf-Nonius CAD4) and centered in the beam path. Standard CAD4 centering, indexing, and data collection programs were utilized [30]. Twenty-five reflections between 10° and 15° in θ were located by a random search pattern, centered and used in indexing. Final cell constants and orientation matrix were obtained by collecting appropriate preliminary data and refined by a least squares fit. During data collection, three intensity standards and three orientation standards were measured at regular intervals to measure the rate of decay of the crystal and to accommodate for crystal movement.

Data were first reduced and corrected for absorption using psi-scans [31] and then solved using the program *SIR-02* [32], which afforded nearly complete solutions for the non-H atoms in all cases. These programs were utilized using the WinGX interface [33]. The models were then refined using *SHELXL-97* [34] first with isotropic and then anisotropic thermal parameters to convergence. The positions and isotropic thermal parameters of the different H-atoms were constrained according to the specifics arranged in the *SHELXL-97* program. This constituted the final model for **2a** and **2c** but it was apparent that two of the C atoms in one of the isopropyl groups in **2b** were disordered. This was accounted for by including atoms at the various sites and refining the occupancies constrained to unity. This resulted in a 81(2)% to 19(2)% disorder in two of the carbon atoms in this isopropyl group.

4. Supporting information available

Crystallographic data for the structural analyses have been deposited with the Cambridge Crystallographic Data Centre, CCDC, Nos. 239506–239508 for compounds **2a–2c** respectively. Copies of this information may be obtained free of charge from: The Director, CCDC, 12 Union Road, Cambridge, CB2 1EZ, UK (Fax: +44-1223-336033); e-mail: deposit@ccdc.cam.ac.uk or www: <http://www.ccdc.cam.ac.uk>).

Acknowledgement

We acknowledge generous financial support by Michigan Technological University.

References

- [1] F.A. Cotton, G. Wilkinson, C.A. Murillo, M. Bochman, *Advanced Inorganic Chemistry*, John Wiley & Sons, New York, 1999.
- [2] F.A. Cotton, B. Hong, *Prog. Inorg. Chem.* 40 (1992) 179.
- [3] G. Jia, R.J. Puddephatt, J.D. Scott, J.J. Vittal, *Organometallics* 12 (1993) 3565.

- [4] M.-C. Brandys, R.J. Puddephatt, *J. Am. Chem. Soc.* 123 (2001) 4839.
- [5] E. Lozano, M. Nieuwenhuyzen, S.L. James, *Chem. Eur. J.* 7 (2001) 2644.
- [6] T. Baumgartner, K. Huynh, S. Schleidt, A.J. Lough, I. Manners, *Chem. Eur. J.* 8 (2002) 4622.
- [7] R.D. Archer, *Inorganic and Organometallic Polymers*, Wiley-VCH, New York, 2001.
- [8] M.A. Fox, D.A. Chandler, *Adv. Mater.* 3 (1991) 381.
- [9] G. Hogarth, *J. Organomet. Chem.* 406 (1991) 391.
- [10] P.W. Wang, M.A. Fox, *Inorg. Chem.* 33 (1994) 2938.
- [11] P.W. Wang, M.A. Fox, *Inorg. Chim. Acta* 225 (1994) 15.
- [12] G. Hogarth, T. Norman, *Inorg. Chim. Acta* 248 (1996) 167.
- [13] E. Zahavy, M.A. Fox, *Chem. Eur. J.* 4 (1998) 1647.
- [14] P.W. Wang, M.A. Fox, *Inorg. Chem.* 34 (1995) 36.
- [15] H.C.E. McFarlane, W. McFarlane, *Polyhedron* 7 (1988) 1875.
- [16] M.E. Peach, C. Bruschka, *Can. J. Chem.* 60 (1982) 2029.
- [17] P.L. Coe, A.J. Waring, T.D. Yarwood, *J. Chem. Soc. Perkin Trans. 1* (1995) 2729.
- [18] T. Rausis, M. Schlosser, *Eur. J. Org. Chem.* (2002) 3341.
- [19] S. Lulinski, J. Serwatowski, *J. Org. Chem.* 68 (2003) 9384.
- [20] S. Lulinski, J. Serwatowski, *J. Org. Chem.* 68 (2003) 5384.
- [21] F. Mongin, M. Schlosser, *Tetrahedron Lett.* 37 (1996) 6551.
- [22] N. Kongprakaiwoot, M.S. Bultman, E. Urnezis, in preparation.
- [23] K.W. Kottsieper, U. Kühner, O. Stelzer, *Tetrahedron: Assymetry* 12 (2001) 1159.
- [24] gNMR, v. 4.1.0, IvorySoft.
- [25] F.H. Allen, *Acta Crystallogr. B* 58 (2002) 380.
- [26] F.H. Allen, O. Kennard, D.G. Watson, L. Brammer, A.G. Orpen, R. Taylor, *J. Chem. Soc. Perkin Trans. 2* (1987) S1.
- [27] G. Hogarth, T. Norman, *Inorg. Chim. Acta* 254 (1997) 167.
- [28] S.J. Higgins, H.S. Jewiss, W. Levason, M. Webster, *Acta Cryst. C* 41 (1985) 695.
- [29] M.A. Bennet, C.J. Copley, A.D. Rae, E. Wenger, A.C. Willis, *Organometallics* 19 (2000) 1522.
- [30] Enraf-Nonius. CAD4 Express Software. Enraf-Nonius, Delft, The Netherlands, 1994.
- [31] A.C.T. North, D.C. Phillips, F.S. Mathews, *Appl. Cryst.* A24 (1968) 351.
- [32] C. Giacovazzo, SIR2002 Program for Crystal Structure Solution, Inst. di Ric. per lo Sviluppo di Metodologie Cristallografiche, CNR, University of Bari, Italy, 2002.
- [33] L.J. Farrugia, *Appl. Cryst.* 32 (1999) 837.
- [34] G.M. Sheldrick, Program for Crystal Structure Refinement, University of Göttingen, Germany, 1997.